Cell, Vol. 104, 605–617, February 23, 2001, Copyright ©2001 by Cell Press

Hyperproliferation and Defects in Epithelial Polarity upon Conditional Ablation of α-Catenin in Skin

Valeri Vasioukhin, Christoph Bauer, Linda Degenstein, Bart Wise, and Elaine Fuchs*
Department of Molecular Genetics and Cell Biology
Howard Hughes Medical Institute
The University of Chicago
5841 S. Maryland Avenue
Chicago, Illinois 60637

Summary

When surface epithelium was conditionally targeted for ablation of α-catenin, hair follicle development was blocked and epidermal morphogenesis was dramatically affected, with defects in adherens junction formation, intercellular adhesion, and epithelial polarity. Differentiation occurred, but epidermis displayed hyperproliferation, suprabasal mitoses, and multinucleated cells. In vitro, α-catenin null keratinocytes were poorly contact inhibited and grew rapidly. These differences were not dependent upon intercellular adhesion and were in marked contrast to keratinocytes conditionally null for another essential intercellular adhesion protein, desmoplakin (DP). KO keratinocytes exhibited sustained activation of the Ras-MAPK cascade due to aberrations in growth factor responses. Thus, remarkably, features of precancerous lesions often attributed to defects in cell cycle regulatory genes can be generated by compromising the function of α-catenin.

Introduction

Adherens junctions (AJs) are intercellular structures prominent in epithelia (Drubin and Nelson, 1996; Gumbiner, 2000). The transmembrane core of the AJ is composed of cadherins, of which E-cadherin is the epithelial prototype. Specialized cadherins (desmogleins and desmocollins) form less dynamic and more robust structures called desmosomes (Kowalczyk et al., 1999). In response to calcium, homotypic interactions specify cell–cell connections (Nose et al., 1988) that are reliant upon the cytoplasmic domain of the cadherin. For desmosomal cadherins, this domain binds plakoglobin and desmoplakin and indirectly associates with intermediate filaments (IFs; Kowalczyk et al., 1999). In contrast, E-cadherin's cytoplasmic domain binds β-catenin, which in turn binds α-catenin (Drubin and Nelson, 1996; Gumbiner, 2000). While β-catenin has been implicated in signal transduction and regulation of adhesion, α-catenin is required to link the AJ to the actin cytoskeleton (Yonemura et al., 1995; Adams et al., 1998; Vasioukhin et al., 2000).

Cell adhesion molecules and their association with the actin cytoskeleton play an important role not only in the maintenance of tissue integrity, but also in proliferation and differentiation. When expressed ectopically in cultured cells, E-cadherin imparts an adhesive, epithelioid morphology. Conversely, disrupting mutations in E-cadherin correlate with invasiveness and metastasis. In some human cancers, including squamous cell carcinomas, underexpression of AJ proteins is often a prognostic marker of poor clinical outcome (Shiozaki et al., 1994; Bagutti et al., 1998; Perl et al., 1998; Yap, 1998), and E-cadherin mutations have been identified in families susceptible to gastric cancer (Guilford et al., 1998).

Cancer cells possess multiple genomic alterations that can make their responses very different from their wild-type counterparts. Although re-expression of E-cadherin or α-catenin can restore epithelioid morphology in vitro, and attenuate tumorigenic properties of cancer cells in nude mice (Watabe et al., 1994; Bullions et al., 1997), embryos lacking specific cadherins die apparently due to tissue degeneration (Larue et al., 1994; Uemura et al., 1996; Carmeliet et al., 1999). These findings have led to the view that when AJ formation is compromised on an otherwise wild-type background, the effects of ablating cell adhesion may be opposite to those in a tumor. Thus, the functions of AJ proteins in general and the consequences of their absence in cancers have been complex and elusive.

Most studies on AJ gene mutations have been conducted on tumors isolated from adult tissues, where additional mutations in protooncogenes have been assumed, albeit not established, to be involved in the phenotype. Mutations in one or more of the members of the Ras-mitogen-activated kinase (MAPK) pathway, or in genes encoding cell cycle proteins such as Rb, are often conjectured as likely candidates responsible for the upregulation in the MAPK pathway and hyperproliferation that are hallmarks of cancer cells. In contrast, mutations in the genes encoding cell adhesion proteins have been attributed to the invasive characteristics (reviewed by Kinzler and Vogelstein, 1996; Yuspa, 1998; Hanahan and Weinberg, 2000). Curiously, mutations in desmosomal proteins have not been associated with cancers, despite their importance in intercellular adhesion.

To assess the importance of AJ proteins on an otherwise wild-type background, and to directly test the significance of the correlation between loss of these proteins and characteristics typically associated with cancer, we have examined the consequences of α-catenin protein ablation in otherwise normal newborn mice. Since α-catenin is required for very early vertebrate embryo development (Kofron et al., 1997; Torres et al., 1997), a conditional knockout approach was needed to explore its function in somatic tissues. In the present study, we used the keratin 14 promoter to activate Cre recombinase and specifically target ablation of α-catenin gene expression in developing surface and oral epithelia.

Our results reveal many unexpected results in the skin of animals whose keratinocyte α-catenin is ablated. In addition to the anticipated loss of AJs, epidermal cell polarity was altered, and hyperproliferation and multinucleate cells were prevalent. The entire epithelium bore

*To whom correspondence should be addressed (e-mail: nliptak@midway.uchicago.edu).

the characteristics of squamous cell carcinoma in situ, a precancerous skin condition. As judged from studies on keratinocytes cultured from α-catenin null epidermis, these features were not a secondary consequence of injury/damage to the skin, but rather appeared to be cell autonomous and independent of intercellular adhesion. We have explored the underlying basis for these most surprising findings, and we have found that in vivo and in vitro, keratinocytes that lack α-catenin display a marked increase in Ras- and mitogen-activated kinase (MAPK) activity. We show that in the absence of α-catenin, E-cadherin complexes with insulin receptor substrate 1 (IRS-1), and that the insulin/MAPK signal transduction pathway is directly responsible for the hyperproliferative phenotype of α-catenin null keratinocytes.

Results

Conditional Knockout of the α-Catenin Gene in Mice

Previously, we engineered K14-Cre recombinase mice and documented the high (near absolute) efficiency and specificity of Cre-mediated recombination in skin epithelial stem cells and their progeny (Vasioukhin et al., 1999). The K14 promoter is strongly upregulated at embryonic day 13.5–14.5 (e14.5), and by birth, most keratinocytes in the skin score positive for the targeted recombination event.

The α-E-catenin gene was isolated from a mouse 129/Sv genomic library, and restriction mapping and partial sequencing identified two exons, the first of which encoded the translation initiation codon and 34 additional amino acid residues lacking known functional domains (Figure 1A). To avoid the risk of generating a truncated α-catenin protein from in-frame ATGs in downstream exons, we engineered our targeting vector such that lox sequences flanked the second exon; removal of this exon generates an early frame shift and translation termination. The targeting vector (Figure 1A) was used to generate two independent RW4 embryonic stem cell (ES) colonies in which a single homologous recombination event had taken place at the α-E-catenin locus (Figure 1B). To delete the floxed neo gene, two clones were transiently transfected with a Cre recombinase gene under the control of the cytomegalovirus (CMV) promoter, and clones from each parental ES line showed successful recombination to remove the neo gene and still retain the floxed second exon. ES technology was then employed to produce germline homozygous mice.

Changes in Cell–Cell Junctions upon α-Catenin Ablation

Animals homozygous for the floxed α-catenin allele displayed no phenotype, indicating that the genomic manipulations had neither created unexpected changes nor interfered with α-catenin function. These animals were bred further to generate newborn animals transgenic for K14-Cre and homozygous for the manipulated α-E-catenin allele. Northern analysis of total e18.5 skin RNA revealed reduced (>10×) α-catenin mRNA (not shown), and Western blot analysis of epidermal proteins detected α-E-catenin protein in wild-type (+/+) and heterozygous (+/−) samples, but not (−/−) samples (Figure 1C). Immunofluorescence verified that the recombination of the α-E-catenin allele was both efficient and keratinocyte specific. While anti-α-catenin antibodies stained wild-type (WT) skin (Figure 1D), staining was absent throughout the epidermis of α-catenin conditional null (KO) skin (Figure 1E). Anti-α-catenin staining in the blood vessels served as a good internal control since the K14-Cre gene is not active in these structures.

Immunoprecipitation and Western analysis revealed no major changes in the levels of other AJ proteins, and E-cadherin retained its association with β-catenin and most other AJ proteins (Figure 1J). These data were consistent with those on α-catenin null blastocysts and cultured cells (Torres et al., 1997; Vasioukhin et al., 2000), verifying that α-E-catenin is not required for the assembly or stabilization of E-cadherin/armadillo family protein complexes.

E-cadherin and other AJ proteins still localized to cell borders in the absence of α-catenin (examples in Figure 1). Prominent cell border staining was also observed with antibodies against proteins specific for desmosomes and tight junctions (not shown). By immunofluorescence microscopy, the only signs of defective cell–cell junctions came from anti-vinculin and phalloidin (actin) staining. However, at the ultrastructural level, intercellular junctions were visibly perturbed (Figure 2). Adherens junctions and continuous epithelial sheets failed to form and many intercellular gaps (asterisks) existed, indicative of unsealed membranes. In addition, fewer desmosomes and tight junctions were observed.

Loss of α-E-Catenin Impairs Hair Development and Causes Major Perturbations in Epidermis

Overt developmental abnormalities were traced to e13.5, when K14 promoter activity is upregulated (Wang et al., 1997). Newborn, conditionally null α-E-catenin pups displayed dramatic defects in their skin and limbs (Figure 3A). Large segments of epidermis were missing and visible peeling occurred at other body sites. Limbs failed to develop fully and the snout was pointed. Mice lacked whiskers and displayed diminished signs of hair follicle morphogenesis, a process which, like limb development, relies upon epithelial–mesenchymal interactions (Hardy, 1992). This provided direct in vivo evidence in support of prior ex vivo studies showing that antibodies against P- and E-cadherins prevent follicle morphogenesis in organ culture (Hirai et al., 1989).

To limit trauma, embryos were used for most experiments. We focused on the epidermal defects, which were dramatic and largely unexpected. In WT epidermis, dividing keratinocytes are normally restricted to the basal layer (BL), and as cells withdraw from the cell cycle, they move outward and differentiate, producing spinous layers (SP), granular layers (GR), and dead stratum corneum cells (SC) (frame 3B). Alpha-catenin null epidermis was thick and disorganized, particularly within the basal layer, where it was difficult to discern the epidermal-dermal boundary (Figure 3). Basal cells were round and spinous cells did not flatten. Intercellular gaps appeared to be weakest at the basal/suprabasal junction, separating the outer layers from the skin (frame D). Despite these abnormalities, morphological signs of differentiation persisted (frame C). Similar features were also seen at the ultrastructural level (Figure 2).

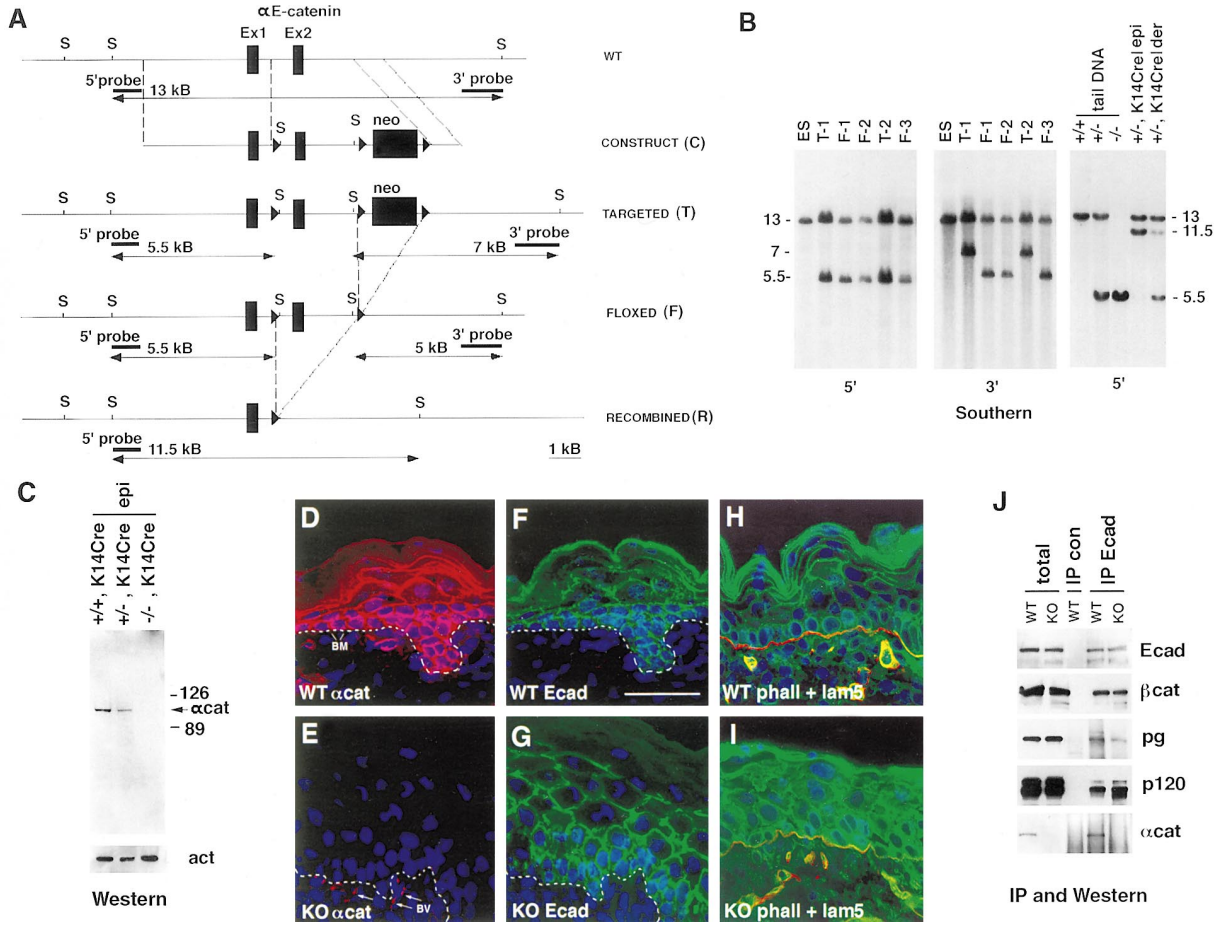

Figure 1. Generation of α-Catenin Null Mice

(A) Four genomic states of the α-E-catenin allele. WT, wild-type allele; T, targeted allele, containing desired recombination event; F, floxed allele, containing loxP sequences flanking α-catenin's exon 2; R, the desired recombined allele, lacking exon 2. Abbreviations: S, SacI; triangles, loxP sequences; Ex1, exon containing ATG translation initiation codon. 5′ and 3′ probes for Southern analysis are denoted by black bars. Fragments expected from SacI digestion and hybridizing to either 5′ or 3′ probe are indicated by the thin double-arrowed lines.

(B) Southern analyses of SacI digested genomic DNAs isolated from: first two blots, positive ES clones before (T) or after (F) transient transfection with CMV-Cre, and last blot, tail or dispase-separated epidermis (epi) and dermis (der) of skins either transgenic for K14-Cre and/or wild-type (+/+), heterozygous (+/−), or homozygous (−/−) for floxed α-E-catenin allele. Sizes of hybridizing bands are in kb.

(C) Western analysis of epidermal proteins. Blots were processed for crossreactivity with α-catenin and β-actin antibodies. Molecular masses are in kDa.

(D–I) Immunofluorescence. Frozen sections of WT and knockout (KO) skins were processed for indirect immunofluorescence and visualized by confocal microscopy. Matched set of frames are from double labelings of same sections stained with DAPI (blue) to label cell nuclei. Primary antibodies were against proteins indicated, with either Texas red (α-catenin or phalloidin) or FITC (E-cadherin) secondary antibodies. Arrows, α-catenin positive blood vessels (BV); dotted line, basement membrane (BM). Bar represents 50 μm.

(J) Cadherin–catenin complexes isolated from e18.5 epidermis of WT and α-catenin null (KO) embryos. Total proteins were extracted and subjected to SDS-PAGE either directly (total) or following immunoprecipitation with antibodies against preimmune sera (con) or E-cadherin. Following electrophoresis, proteins were subjected to Western analysis using the antibodies indicated.

Interestingly, mitotic figures were detected throughout α-catenin null epidermis (Figure 3, frames E and F). In some regions, disorganized masses of keratinocytes were seen within the dermis (Figure 3, frames G–K). These dermal epithelial masses displayed morphology and differentiation characteristic of epidermis and not hair follicles. This feature was consistent with the observed block in hair follicle morphogenesis. Masses were particularly large in areas where skin was devoid of surface epidermis, suggesting that these masses arose from invagination of surface epithelium into dermis.

KO keratinocytes were quite frequently binucleate and unusually large, features observed in both internalized epithelial masses and in epidermis (Figure 3C). A reflection of aberrant mitoses, multinucleation was confirmed by analysis of in vitro cultures: 22% ± 7% of null basal keratinocytes versus 4% ± 3% of wild-type basal keratinocytes. Taken together, the morphology consisting of hyperproliferation, defects in cell polarity, abnormally large and multinucleated keratinocytes, and mitoses in multiple cell layers and in the dermal epithelial masses bore a resemblance to a precancerous condition, which in humans is known as squamous cell carcinoma in situ (Freedberg et al., 1999).

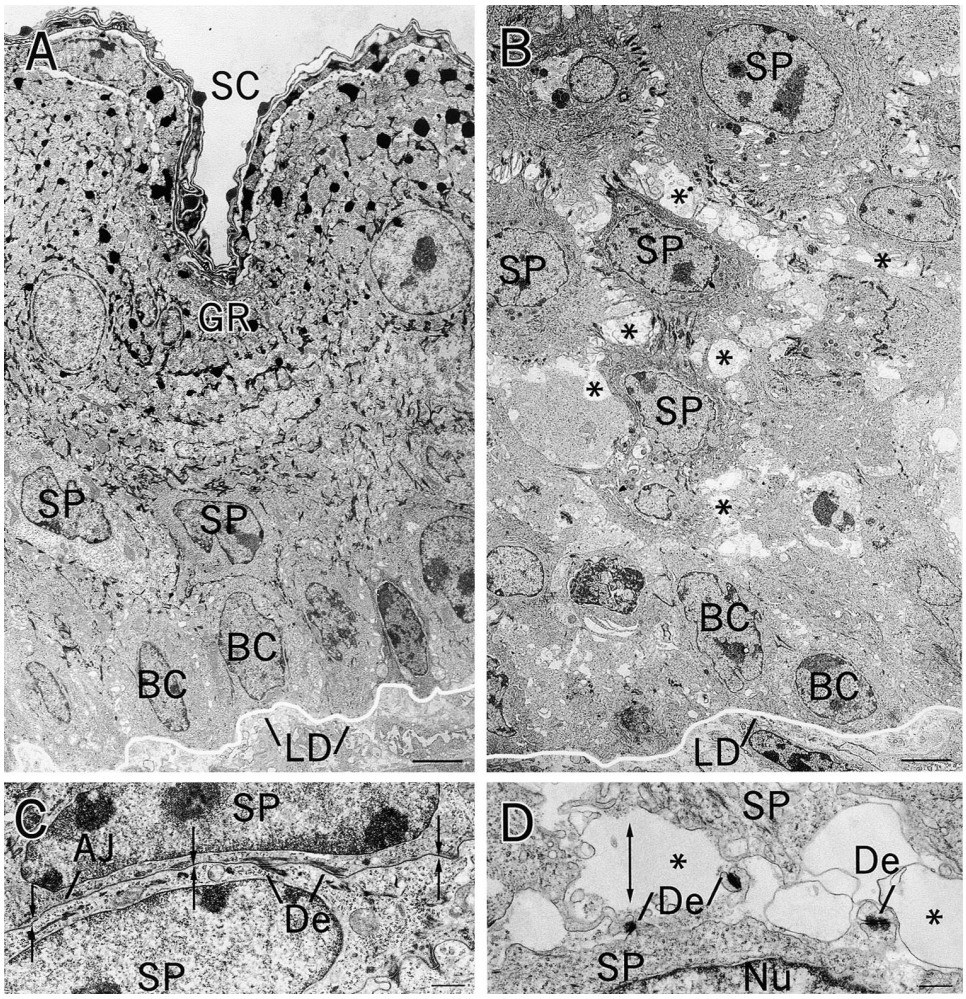

Figure 2. Intercellular Junctions Are Impaired in α-Catenin Null Epidermis

Skins from e18.5 WT (frames A and C) and KO (frames B and D) mice were processed for electron microscopy.

(A) Note columnar basal cells (BC) and flattened spinous cells (SP). White line denotes lamina densa (LD), demarcating the dermal/epidermal border.

(B) Note loss of columnar morphology in basal cells and disorganized suprabasal cells. No adherens junctions or tight junctions were detected, and membranes did not seal (asterisks and double arrows in [B] and [D]). A few desmosomes were still seen in the lower spinous layer, but numbers were reduced by more than 10-fold (D). Additional abbreviations: De, desmosome; AJ, adherens junction; SC, stratum corneum; GR, granular layer; Nu, nucleus; double arrows in (C), perfectly sealed membrane. Bar represents 2 μm in (A) and (B) and 200 nm in (C) and (D).

Hyperproliferation in α-Catenin Null Epidermal Cells Is Independent of Defects in Cell–Cell Adhesion

We next used immunofluorescence microscopy to examine the expression of epidermal markers of differentiation, extracellular matrix, cell-substratum attachment, and proliferation (Figure 4). Antibodies against well-characterized markers of terminal differentiation, including involucrin, filaggrin, and loricrin, revealed patterns indistinguishable between control and mutant skin (not shown). Some patches of (−/−) epidermis were absent for K1, one of the two major keratins expressed in spinous cells (frame A). Despite a few local perturbations, however, the biochemical program of differentiation was still operative. Epidermal differentiation-specific markers were also detected in the epithelial masses; these masses did not stain with antibodies against hair keratins (monoclonal AE13), inner root sheath markers (monoclonal AE15), or Lef1, an early marker of hair follicle morphogenesis (data not shown). These findings were consistent with an epidermal origin of these masses.

The inner epidermal layers seemed particularly affected in α-catenin null epidermis. Anti-K5 staining extended aberrantly into the suprabasal layers (frames B and C). Antibodies against the basement membrane marker laminin 5 revealed atypical deposition in upper layers and gaps in staining along the basement membrane (frame D). Abnormalities were also seen in β4-integrin, normally confined to the juncture where epidermis adheres to basement membrane. In KO epidermis, staining was diffuse at the basal surface, and often at lateral and apical surfaces of basal cells (frame E).

Additional immunofluorescence microscopy revealed potential abnormalities in epidermal proliferation. Anti-

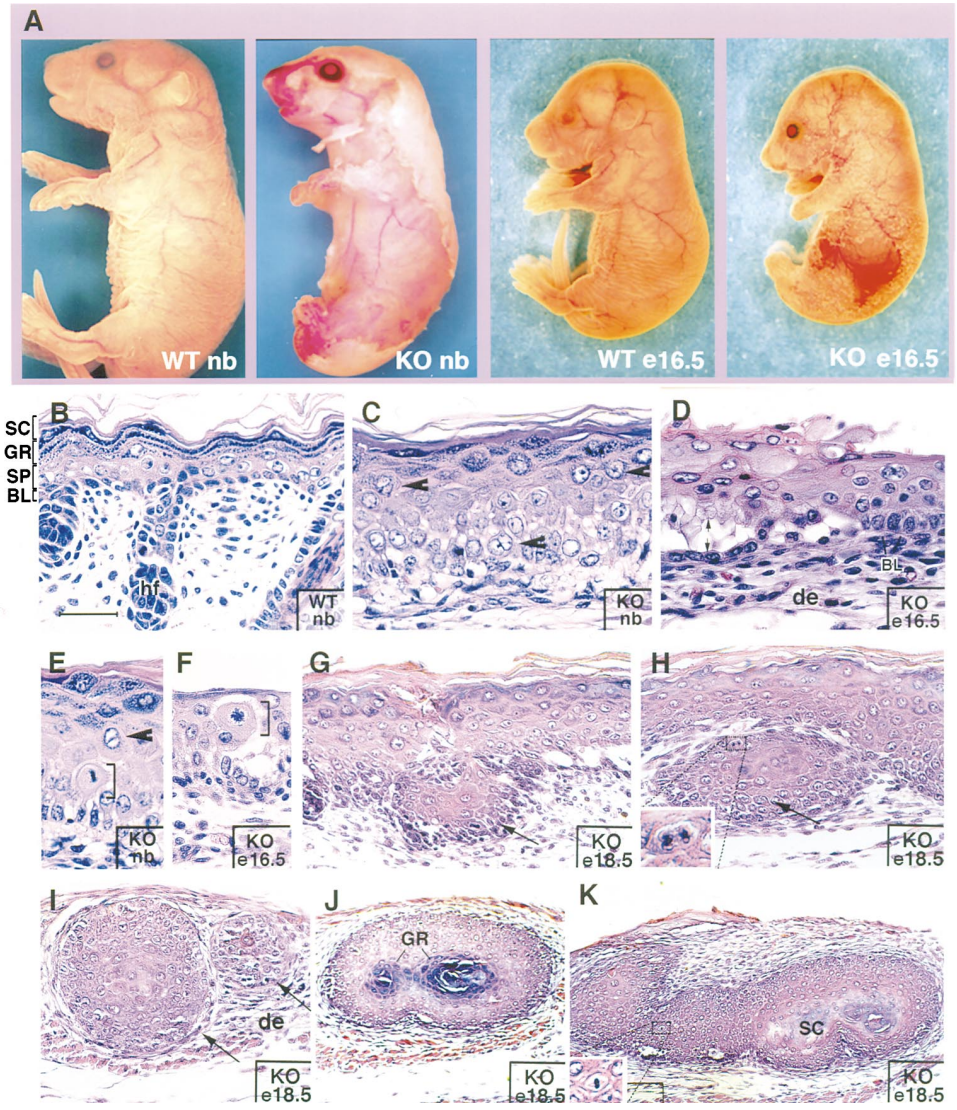

Figure 3. Visible and Histological Abnormalities in α-E-Catenin Null Skin

(A) Representative α-catenin null (KO) and controls (WT) from newborn (nb) and e16.5 litters.

(B–K) Hematoxylin- and eosin-stained skin sections. Abbreviations: BL, basal layer; SP, spinous layers; GR, granular layers; SC, stratum corneum; de, dermis; hf, hair follicle. Arrowheads denote seemingly multinucleate cells; arrows denote epidermal invaginations resulting in dermal masses of epithelium beneath the skin surface. Insets in (H) and (K) denote mitoses, prevalent within these masses. Brackets denote suprabasal mitoses. Bar in (B) represents 80 μm in (B)–(F), 120 μm in (G)–(I), and 240 μm in (J) and (K).

bodies against keratin 6 did not stain WT epidermis, but did stain throughout the suprabasal layers of KO epidermis (frame E) and within interior layers of associated epithelial masses (frame F). In epidermis, K6 is a differentiation marker typically seen under conditions of hyperproliferation (Sun et al., 1984; Stoler et al., 1988). Antibodies against the proliferative marker Ki67 labeled epithelial masses extensively as well as all layers of KO epidermis (frames G and I); in contrast, WT epidermis showed labeling that was restricted to the inner most basal layer (frame H).

To assess whether these unexpected changes might be a result of tissue injury or a mandatory consequence of defective intercellular adhesion, we compared skin from α-catenin null animals with skin conditionally targeted for loss of desmoplakin (DP), a desmosomal protein necessary for linking cytoskeleton to desmosomes (details of the DP KO phenotype to be published elsewhere). Both animals showed severe intercellular adhesion defects with comparable degrees of epidermal separations and skin peeling. However, in striking contrast to α-catenin null epidermis, DP KO epidermis displayed normal anti-Ki67 labeling, K6 staining, and epidermal polarity without noticeable internalized epithelial masses (example in frame J). This is compelling evidence that defects in epidermal polarity and cell proliferation are a direct and specific consequence of α-E-catenin ablation.

The hyperproliferative and invasive characteristics of α-catenin null epidermal cells were also observed in

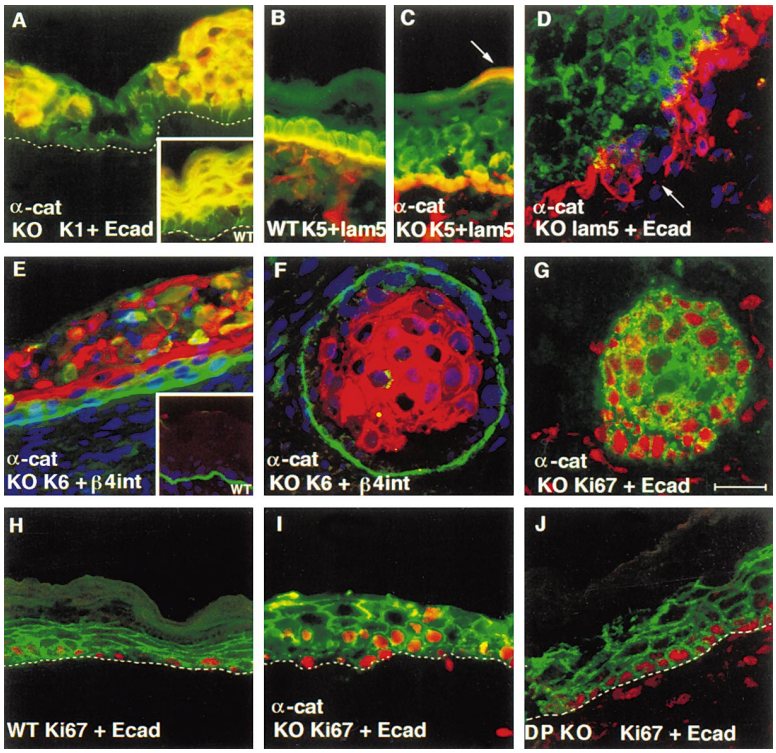

Figure 4. Regulated Differentiation, but Perturbations in Polarity and Proliferation in α-Catenin Null Epidermis

Immunofluorescent staining of WT and KO skins (either α-catenin null or desmoplakin null). Insets depict WT staining patterns. Primary antibodies were against proteins indicated at lower left of frames. Secondary antibodies were: FITC for E-cadherin (typically at cell borders of all epidermal layers), K5, and β4-integrin (typically only in basal cells); Texas red for keratin 1 (an epidermal terminal differentiation marker normally found in suprabasal epidermal cells), laminin 5 (a basement membrane component), keratin 6 (typically seen in suprabasal layers of hyperproliferating epidermis), and Ki67 (a nuclear antigen marker of proliferating cells). Arrow in (C) denotes laminin 5 staining in suprabasal KO cell, not seen in WT; arrow in (D) denotes break in basement membrane, not seen in WT. Dotted lines denote epidermal-dermal borders. Bar represents 30 μm for (F) and (G) and 50 μm for (A)–(E) and (H)–(J).

vitro (Figure 5). Pure populations of keratin 5/14 positive, primary epidermal keratinocytes were readily obtained by isolating the epidermis from dispase-treated KO and WT littermate skins, and culturing the cells in the presence of 15% serum and insulin to favor keratinocyte growth (Vasioukhin et al., 2000). Control littermate keratinocytes formed continuous epithelial sheets when at high density in normal, calcium-containing medium (frame A). In contrast, KO keratinocytes were rounder and overgrew the monolayer, piling into foci characteristic of tumor cells (frames B and C; reviewed by MacPherson, 1970). Anti-K5 and anti-K14 staining confirmed the keratinocyte origin of the foci (frames D and E). The impairment of contact inhibition was also reflected in the downregulation of p27 (frame F), a cyclin-dependent kinase inhibitor implicated in contact inhibition (St Croix et al., 1998).

Loss of α-catenin did not seem to affect the ability of keratinocytes to traverse a membrane in migration assay chambers, at least under the rich media conditions used here (frame G). However, when membrane filters were precoated with Matrigel (extracellular matrix), KO keratinocytes exhibited an increased ability to break down the matrix and traverse the filter after a chemoattractant (medium conditioned by fibroblast feeder cells) was added to the bottom chamber (frame G). These findings were intriguing given the interruptions seen in the basement membrane of α-catenin null epidermis.

Alpha-catenin null mouse keratinocytes displayed additional features characteristic of transformed cells. In contrast to WT keratinocytes, which required a fibroblast feeder layer for long term growth (>7 days) in high calcium, KO keratinocytes grew equally well in the presence or absence of a feeder layer (Figure 5H). Moreover, the KO cells grew abnormally fast. In contrast to the littermate controls, which were confluent at ~200,000 cells per well and doubled every ~24 hr, KO cells were poorly contact inhibited and prior to confluence, doubled every ~13 hr. Interestingly, this difference persisted even in low calcium medium, i.e., under conditions where AJs and desmosomes do not form (Figure 5I). This result strengthens the view that hyperproliferation is a direct consequence of the α-catenin null state and not one that arises secondarily from a loss of intercellular adhesion.

Finally, we examined the ability of WT and KO keratinocytes to reenter the cell cycle after withdrawing serum and insulin supplements from the culture medium. 14 hr after readdition of serum and insulin, cells were trypsinized and subjected to fluorescence-activated cell sorting (FACS). KO keratinocytes were significantly more responsive to growth/serum factors than their WT counterparts; more than twice the number of KO cells progressed from G0/G1 to G2/M during this time (Figure 5J).

Sustained Activation of Ras-MAPK as a Consequence of α-Catenin Ablation

To address how loss of α-catenin might lead to hyperproliferation, we examined several candidate signal transduction pathways that could be involved. A priori, in the absence of α-catenin, β-catenin's stability might increase, enabling it to influence gene transcription regulated by the Lef1/Tcf family of DNA binding proteins. However, we did not detect major differences in the levels of β-catenin associated with E-cadherin (see Figure 1J) or in overall β-catenin levels (see below). Moreover, using an antibody that can detect nuclear β-cat-

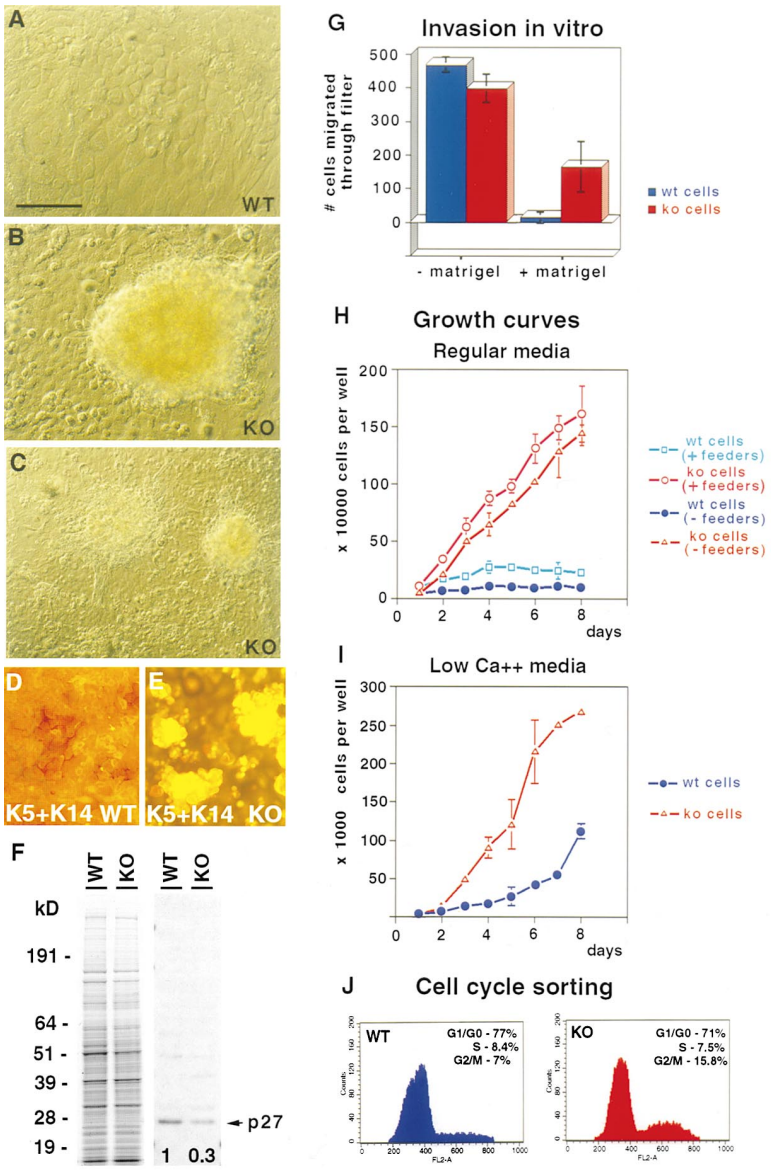

Figure 5. Alpha-Catenin Null Keratinocytes In Vitro Exhibit Impaired Contact Inhibition, Invasion through Extracellular Matrix, and Hyperproliferation

Epidermis from skins of either α-catenin conditional null animals (KO) or wild-type littermates (WT) was separated from dermis, and pure populations of K14/K5 expressing keratinocytes were cultured as described previously (Vasioukhin et al., 2000).

(A–C) Differential interference contrast (DIC) images of WT (A) and KO cells (B and C), cultured on a mitomycin C-treated fibroblast feeder layer in the presence of high calcium medium and photographed 10 days after reaching confluence. Note the presence of an epithelial sheet of WT keratinocytes that show sealed membranes at intercellular junctions, evidence of contact inhibition. In contrast, KO keratinocytes are round and pile up into multilayered foci, evident at both high (B) and low (C) magnification. These foci form irrespective of whether KO keratinocytes are grown on feeders or not.

(D–E) Indirect immunofluorescence microscopy of WT (D) and KO (E) keratinocytes cultured as above and labeled with anti-K5 (green) and anti-K14 (red).

(F) Protein extracts from KO and WT keratinocytes were subjected to Western blot analysis with an antibody against p27, known to be upregulated upon E-cadherin-mediated cell–cell adhesion (St. Croix et al., 1998). Shown also is Coomassie blue staining to illustrate equivalent loadings of samples.

(G) Migration and invasion assays were performed by using Matrigel Invasion Chambers, with or without extracellular matrix, as described in Experimental Procedures. Without Matrigel, roughly equivalent numbers of keratinocytes migrated from the top to the bottom chamber in response to the attractant (fibroblast-conditioned medium); with Matrigel, an equivalent number of cells attached, but KO cells displayed a marked increase in their ability to invade the extracellular matrix and move to the bottom chamber.

(H) Growth curves of WT and KO keratinocytes cultured in the presence of high calcium, serum, and insulin supplemented medium, ± fibroblast feeder cells (see Experimental Procedures for details). Under the conditions employed, WT cells require a feeder layer; they reached confluence 4 days after cell counting was initiated. In contrast to WT cells, KO cells grew more rapidly, and independently of the feeder layer. Error bars reflect the standard deviation within each set of triplicate wells counted.

(I) Growth curves of WT and KO keratinocytes cultured in the presence of low calcium medium, i.e., conditions that prevent intercellular junction formation. (Note: under low calcium conditions, mouse keratinocytes are normally cultured in the absence of a feeder layer.) Note that KO cells still grew more rapidly than WT cells.

(J) FACS analyses of WT and KO keratinocyte cultures first placed in serum and insulin-free medium for 48 hr and then supplemented with serum and insulin for 14 hr. Note that after stimulation, fewer WT cells had progressed to the G2/M phase of the cycle by 14 hr. At later times, WT cells did progress through the cell cycle and proliferate, verifying that this difference is a reflection of a lag in responding to serum/insulin supplements. Bar represents 120 μm (A,B, D, and E); 240 μm (C).

enin (U. Gat, B. Merrill, and E. F., unpublished data), we did not detect nuclear β-catenin in α-catenin null epidermis (not shown). Finally, α-catenin null epidermis did not reveal activation of the TOPGAL reporter gene, which relies upon stabilized β-catenin (DasGupta and Fuchs, 1999). An overall paucity of TOPGAL expression in α-catenin null/TOPGAL mice correlated with the paucity of hair follicles, which typically show TOPGAL activity. Taken together, these findings made it unlikely that transactivation of β-catenin/Tcf/Lef1 regulated genes was the underlying cause of hyperproliferation in α-catenin null skin epithelium.

In searching further for a molecular explanation for the unanticipated hyperproliferation of KO epidermis, we discovered that antibodies against activated (phosphorylated) MAPK displayed enhanced and specific staining only in the α-catenin null state (Figure 6). Such changes were also seen in the tumor-like masses of KO skin (not shown). Sustained MAPK activation was confirmed by Western blot analysis and it also occurred

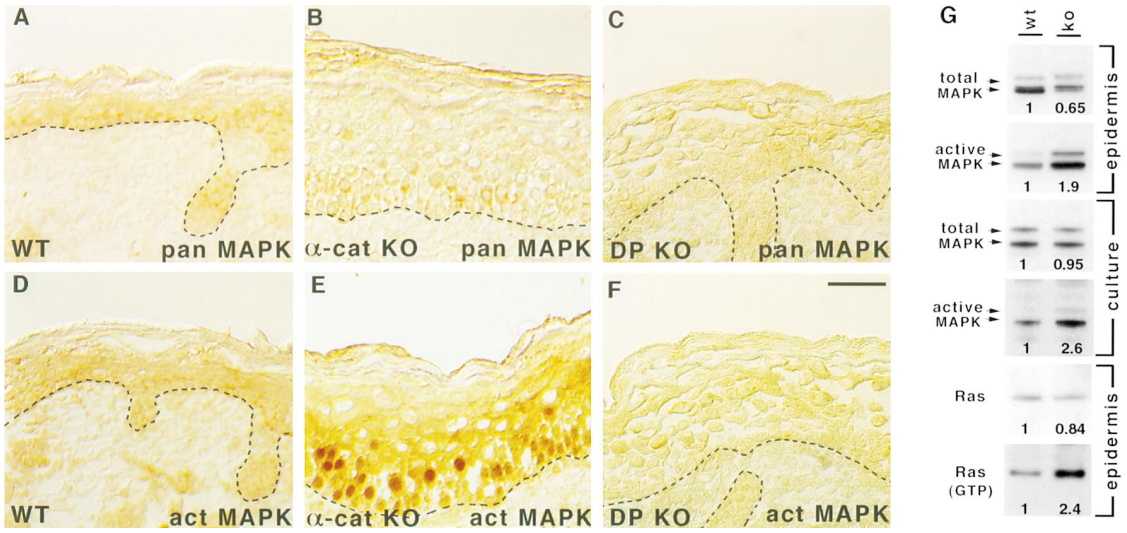

Figure 6. Sustained Activation of Ras-MAPK Cascade in α-Catenin Null Epidermis and Cultured Keratinocytes

(A–F) Frozen sections of WT (A and D), α-catenin KO (B, E), and desmoplakin KO (C and F) skins were processed for immunohistochemistry using panel antibodies (pan MAPK) against Erk1/2 (A–C) or specific antibodies (act MAPK) for activated (Thr202/Tyr204) Erk1/2 (D–F). Note that upon activation, Erk1/2 concentrates in the nucleus. Dotted lines denote epidermal-dermal borders. Bar represents 50 μm.

(G) Immunoblot analyses and Ras activity assays. Total proteins were extracted from the epidermis or from cultured epidermal keratinocytes of wt and ko animals. In the top five panels, proteins were resolved by SDS-PAGE and subjected to immunoblot analyses with antibodies against all Erk1/2 isoforms (total MAPK), the phosphorylated, i.e., activated, Erk1/2 forms (active MAPK), or Ras as indicated to the left of each panel. In the bottom panel, GTP bound Ras was detected using a GST pulldown assay. Numbers below bands represent a quantitation of the results and shows the fold difference in densities between the bands in WT (arbitrarily set at 1.0) versus KO cells.

in KO cultures, indicating that the effect is cell autonomous (Figure 6G). Notably, sustained MAPK activation was not observed in epidermis conditionally targeted for desmoplakin (Figures 6C and 6F). This argues further against the notion that Ras-MAPK activation in α-catenin null epidermis is simply a wound-healing response induced by perturbations in epidermal cell–cell adhesion.

GTP bound Ras was the most central effector of Erk1/2 MAPKs that seemed relevant to the phenotype observed. As judged by an assay measuring the ability of activated Ras to bind to the downstream effector kinase Raf1 (Herrmann et al., 1995), we observed a substantial (>2×) increase in the levels of activated Ras in the epidermis of α-catenin null mice as compared to their control littermates (Figure 6G).

The Relevance of Sustained Ras-MAPK Activation to α-Catenin Null-Mediated Growth Differences

Ras isoforms are key regulators of cell growth, and mutations that lead to sustained activation of Ras/Erk MAPKs predispose epidermis to malignant conversion (Yuspa, 1998; Balmain and Harris, 2000; Wang et al., 2000). The Ras-MAPK pathway is activated by growth factors that bind and activate receptor tyrosine kinases. Since we typically add insulin and serum to our mouse keratinocyte cultures, we first examined how each of these additives influenced the kinetics of MAPK activation. As shown in Figure 7A, enhanced MAPK-phosphorylation was observed within minutes after treatment with insulin. The activated MAPK response was significantly (>8×) more pronounced in the KO cells, as was the ability of insulin to stimulate Ras activation. These data provided a direct link between the α-catenin null state, hyperproliferation, increased insulin sensitivity, and enhanced Erk MAPK and Ras activation.

KO keratinocytes also displayed increased sensitivity to insulin-like growth factor 1 (IGF-1), but not to epidermal growth factor (EGF) or to serum (Figure 7A). The response appeared to be specific for MAPK activation, as KO and WT keratinocytes treated with insulin and/or IGF-1 displayed similar activation levels of the phosphoinositide-3 activatable kinase, AKT (Figure 7A; shown are data for insulin). This was somewhat surprising since in mesenchymal cells, PI3K activation plays a major role in insulin-mediated metabolic responses (Chan et al., 1999).

The increased sensitivity to insulin and IGF-1 was not associated with an increase in receptor tyrosine kinase levels and/or activity, but rather it appeared to involve a change in the propagation of the signal at a downstream step (Figure 7A). The interacting protein insulin receptor substrate 1, or IRS-1, associates with activated insulin and IGF-1 receptors and upon tyrosine phosphorylation, it can bind both Grb2-SOS (the guanine nucleotide exchange factor for Ras) and phosphoinositide-3 kinase, necessary for AKT activation (Myers et al., 1994; Chan et al., 1999). Recently, it was discovered that IRS-1 can interact with E-cadherin in colorectal cancer cells (Playford et al., 2000). We found that this interaction also occurred specifically in α-catenin null and not WT keratinocytes and that the IRS-1 in the complex becomes specifically tyrosine phosphorylated upon treatment with insulin. Thus, when protein extracts from insulin-treated KO keratinocytes were immunoprecipitated with E-cadherin antibodies, and subjected to SDS-PAGE and

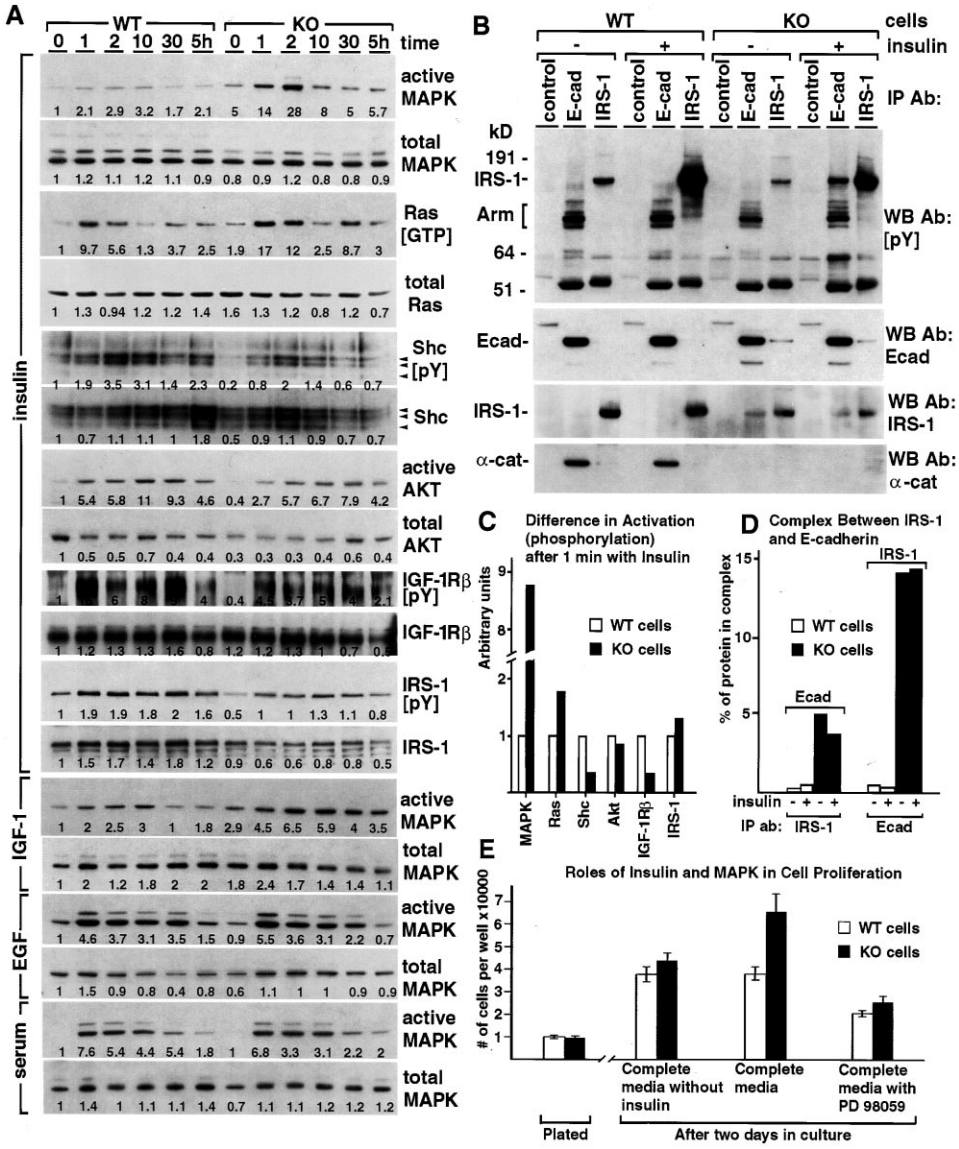

Figure 7. The Growth Advantage and Sustained MAPK Activation of α-Catenin-Deficient Keratinocytes Observed In Vitro Arises from an Altered Response of KO Cells to Insulin

(A) Measurements of activated MAPK, Ras, AKT, Shc, and tyrosine kinase receptors in response to insulin. WT and KO cells were growth arrested for 24 hr in medium lacking serum and insulin. To stimulate cells, serum or one of several growth factors (insulin, IGF-1, or EGF) was added to the medium as indicated. At t = 0, 1, 2, 10, 30 min, or 5 hr after supplementing the medium, proteins were isolated and subjected to Western blot analysis with the antibodies indicated. In some cases, extracts were immunoprecipitated with antibodies prior to Western analyses. Antibodies against the phosphorylated forms of the proteins are those against the active forms.

(B) Association of insulin receptor substrate 1 (IRS-1) with E-cadherin. Total proteins were isolated from WT and KO keratinocytes cultured for 24 hr in the absence of serum/insulin and then stimulated with 10 μg/ml insulin for 2 min. Extracts were used to immunoprecipitate indicated proteins with control serum or with antibodies against E-cadherin or IRS-1. The precipitates were then analyzed by SDS-PAGE and Western blots were probed with antibodies (Ab) against anti-phosphotyrosine (pY), E-cadherin, IRS-1, or α-catenin. Note: the satellite band recognized by anti-E-cadherin antibodies in the anti-E-cadherin immunoprecipitate is a degradation product of E-cadherin that was always more prominent in the α-catenin null cells.

(C) Quantitation of the difference in activation (phosphorylation) of indicated proteins extracted from WT and KO cells after stimulation with insulin for one minute. Data were obtained from Western blots shown in (A). Data were normalized based upon the amounts of total (activated + nonactivated) protein in each sample, and represent the fold difference in activation (phosphorylation) of the proteins. WT values at time 0 were arbitrarily set at 1.0.

(D) Quantitation of complex formation between IRS-1 and E-cadherin. Data were obtained from the experiment outlined in (B). Data show the percentages of E-cadherin immunoprecipitated with IRS-1 antibodies and, conversely, IRS-1 immunoprecipitated with E-cadherin antibodies.

(E) Cell proliferation assay. WT and KO cells were plated in the presence of 15% serum, 5 μg/ml insulin, and high calcium. Parallel cultures were plated in similar medium, but either without insulin or in the presence of the MAPK inhibitor PD98059. Comparable numbers of KO and WT cells attached after plating overnight ("plated"). After two days in culture, cells were trypsinized and counted. Error bars reflect the standard deviation within each set of six wells counted.

anti-phosphotyrosine Western blot analysis, tyrosine-phosphorylated IRS-1 was detected (first blot of Figure 7B). Anti-IRS-1 antibodies also immunoprecipitated E-cadherin in KO but not WT cells (second blot of Figure 7B). In this case, complexes were detected irrespective of whether insulin had been added to the medium.

A summary of these data is provided in Figures 7C and 7D. The findings demonstrate that in KO keratinocytes treated with insulin, IRS-1 is phosphorylated and forms a complex with E-cadherin/β-catenin, thereby providing a link between insulin/IGF-1 receptors and these AJ proteins. Downstream from these changes is an increase in the activation of Ras and MAPK.

Finally, we examined whether the enhanced proliferation in KO keratinocytes was attributable to their increased sensitivity to the insulin in the culture medium. When insulin was withheld from the serum-supplemented growth medium, the growth difference between KO and WT cultures was no longer observed (Figure 7E). This difference was also obliterated upon treatment of the cells with PD98059, a potent inhibitor of the MAPK pathway (Figure 7E). Thus, while inhibition of Erk MAPK attenuated the growth of both KO and WT cells, it erased the growth advantage of the KO cells in complete medium. Thus, sustained activation of Erk MAPKs appeared to be necessary for the proliferative advantage of α-catenin null keratinocytes, and in culture, this difference was dependent upon insulin.

Discussion

Unexpectedly Broad Effects for a Single Dysfunctional Gene: More to α-Catenin than Adherens Junction Formation

Disruption of the α-catenin gene in embryonic mouse cells leads to a preimplantation defect in trophoblast epithelium, and the carboxyl terminus of the protein is required for this function in vivo (Torres et al., 1997). Alpha-catenin is also required for AJ formation in vitro and for reorganization of actin filaments during epithelial sheet formation (Adams et al., 1998; Vasioukhin et al., 2000). Our data now extend these prior observations to α-catenin null epidermis, which displays abnormalities in intercellular adhesion and actin organization.

The remarkable finding of the present study is that dysfunction of α-catenin so profoundly changes the epidermis and adorns it with many of the characteristics of a precancerous state known as squamous cell carcinoma in situ. The effects went well beyond the mere loss of AJ formation to include uncontrolled growth, multinucleate cells, partial loss of epithelial polarity, and the appearance of large epidermal masses in the dermis. Since the entire epithelium of the α-catenin null skin was affected shortly after the conditional targeting event was induced, these dramatic and sweeping changes must be primary, i.e., attributable solely to the loss of this protein.

A correlation between AJ dysfunction, tumor invasion, and metastasis has long been known. At first glance, given the substantial evidence that links epithelial cancers with a reduction in AJs, it may not seem so surprising that α-catenin ablation in skin epidermis leads to many of the features of precancerous squamous metaplasia. In fact, however, the prevailing notion has been that a reduction in cell–cell adhesion is but one component of the tumorigenic phenotype, which collectively requires the dysregulation of additional oncogenes. Mutations in adhesion genes have been assumed to be important largely for detachment and relocation of tumor cells and not sustained hyperproliferation or generation of multinucleate cells.

While attractive, the above hypothesis does not provide an adequate explanation for why mutations in desmosomal cadherins and/or their cytoskeletal linker proteins have not been associated with cancers, despite their equally important role in intercellular adhesion. Our results uncovered an intriguing difference between mutations in AJ versus desmosomal proteins. Despite similar severity in intercellular adhesion defects, α-catenin mutations resulted in uncontrolled growth, whereas desmoplakin mutations did not. These findings underscore that the explanation resides within the specific adhesion gene mutated, rather than the reduction in intercellular adhesion per se.

Several lines of evidence suggest that the functions of AJ proteins might extend beyond a mere adhesive role to include epithelial polarity and growth. Thus, for example, transfections of AJ genes into carcinoma cell lines rescued microvilli formation and apical/basal polarity in vitro (Watabe et al., 1994), and/or attenuated their ability to form tumors in nude mice (Bullions et al., 1997; see also Nathke et al., 1994; St Croix et al., 1998). In opposition of a growth regulatory role, however, has been the knockouts of several cadherin genes, which cause early embryonic lethality and tissue degeneration (Larue et al., 1994; Uemura et al., 1996; Carmeliet et al., 1999; see also Torres et al., 1997). Our studies demonstrate that the effects on hyperproliferation and epithelial polarity can be segregated from those on cell–cell adhesion. In vitro, the difference in proliferative rates between α-catenin null and control keratinocytes existed even under conditions where cell–cell adhesion was suppressed. Thus, a novel importance can be assigned to α-catenin that goes beyond its well-established role in intercellular adhesion.

A Possible Molecular Basis for the Potent Hyperproliferative Effects of α-Catenin Ablation

A priori, a number of possible mechanisms could account for how a loss of α-catenin might lead to hyperproliferation. An important insight came from our discovery that sustained activation of the Ras-MAPK pathway is coupled to a loss in α-catenin. This striking result places α-catenin ablation upstream of this cascade, and provides an explanation for the potent hyperproliferative effects of α-catenin ablation in skin. In epidermis in vivo, the sustained activation of Erk1/2 MAPKs correlated strongly with uncontrolled growth and not loss of intercellular adhesion. Thus, while ablation of desmoplakin and α-catenin each resulted in a dramatic impairment of intercellular adhesion, only the α-catenin null epidermis showed marked hyperproliferation and phospho-MAPK antibody staining. In epidermal keratinocytes in vitro, hyperproliferation could be blocked with Erk1/2 pathway inhibitors, suggesting that sustained activation of MAPK is responsible for the uncontrolled growth of these cells.

How does loss of α-catenin lead to sustained MAPK activation? Although many signal transduction pathways converge at this point, the activation of transmembrane integrins and tyrosine kinase growth factor receptors are known to influence MAPK activation and lead to reduced intercellular adhesion in keratinocytes and other epithelial cells (Hodivala and Watt, 1994; Kinch et al., 1995; Higgins et al., 1998; Espada et al., 1999; von Schlippe et al., 2000). Although we did not detect increased migration in cultured α-catenin null keratinocytes, integrin expression extended suprabasally and their localization was apolarized in epidermis in vivo. Whether integrin activation is altered in α-catenin null skin and whether this accounts for some of the effects observed needs to be explored in more depth.

While a direct link to integrin signaling has not yet surfaced, we accumulated substantial evidence directly linking E-cadherin/β-catenin complexes to growth factor tyrosine receptor pathways. In α-catenin null keratinocytes, the hyperproliferative response and sustained MAPK activation were clearly coupled, and directly attributable to the presence of insulin added as a key growth supplement to the culture medium. In vivo, additional growth factors may play a role in this process.

Our studies indicate that the perturbation in growth factor response occurs downstream of IR/IGFR activation and appears to be rooted in an altered interaction between IRS-1 and E-cadherin. At present, we don't know how this leads to activation of the Ras-MAPK pathway, but other investigators have shown that activated IRS-1 can directly bind to the Ras guanine nucleotide exchange factor Grb2-SOS. Another downstream IRS-1 effector, Fyn, may also be involved as activated Fyn levels were higher in α-catenin null epidermis in vivo and dominant negative Fyn erased the difference in MAPK activity between KO and WT keratinocytes in vitro (data not shown). However, these signal transduction pathways are complex and often intersecting and additional mechanisms for activation of the Ras-MAPK cascade may be involved.

In summary, our data reveal that loss of α-catenin not only compromises intercellular adhesion, but also leads to an altered response of keratinocytes to several different growth factors that activate membrane bound tyrosine kinase receptors on the surface of epidermal cells. At least one growth factor receptor pathway leading to sustained activation of Ras-MAPK is directly coupled to E-cadherin/β-catenin complexes through IRS-1. In vitro, without insulin, the growth advantage of α-catenin null keratinocytes is obliterated, suggesting that this pathway is likely key in manifesting the uncontrolled growth response of the α-catenin null state. The ability of α-catenin null mutations to not only perturb AJs, but also to constitutively activate Ras-MAPK provides a basis for why we observed more dramatic effects with α-catenin ablation in skin epithelium than has been observed with classical MAPK activating oncogenes.

Experimental Procedures

Histology, Western Blot Analysis, and Immunofluorescence

Protein extractions, Western blot, and immunoprecipitation analyses were performed as described (Ozawa and Kemler, 1998). For routine histology, tissues were fixed in Bouin's fixative, processed, and embedded in paraffin. Sections (5 μm) were stained with hematoxylin and eosin, examined and photographed using an Axiophot microscope (Carl Zeiss, Thornwood, NY). For immunofluorescence, frozen sections of tissues or cells on the glass coverslips were fixed in 4% paraformaldehyde in PBS for 10 min and were subjected to double indirect immunostaining (Gallicano et al., 1998) and analyzed using a confocal microscope LSM 410 (Carl Zeiss, Thornwood, NY).

Primary antibodies used were: E-cadherin (Zymed, San Francisco, CA; Sigma Chemicals, St. Louis, MO); β-catenin, Shc, phosphorylated tyrosine (pY), and p120 (Transduction Laboratories, Lexington, KY); laminin 5 (Sigma, St. Louis, MO); keratin 5 (1:400, 10); keratin 6 (1:500, Dr. P. Coulombe); keratin 10 (Babco, Richmond, CA); Ki67 (Vector laboratories, Burlingame, CA); β4-integrin and p27kip (Pharmingen, San Diego, CA); α-catenin (Sigma, Transduction Laboratories); pan Ras (Oncogene Research, Cambridge, MA); IRS-1 and IGFRβ (Santa Cruz, Santa Cruz, CA); MAPK and phosphorylated (activated) MAPK, AKT and phosphorylated AKT (New England Biolabs, Beverly, MA). Dilutions were according to the manufacturer's recommendations. Fluorescence-conjugated secondary antibodies were from Jackson ImmunoResearch (West Grove, PA).

Separation of Epidermis, Primary Keratinocytes Isolation, and Culture

Separation of epidermis and isolation of keratinocytes were as described (Wang et al., 1997). Mouse keratinocyte culture conditions for high calcium with fibroblast feeder layers were as for human epidermal keratinocytes with the exception that we typically omit EGF, leaving insulin as the primary growth factor additive (Rheinwald and Green, 1975). 24 well plates were prepared with or without a mitomycin C-treated fibroblast feeder layer and seeded with 25,000 keratinocytes per well. For low calcium, 5000 keratinocytes per well were seeded and cells were cultured in the absence of a feeder layer as previously described (Wang et al., 1997). Media was changed daily for the first 6 days and every 12 hr on the 7th and 8th days as necessary. For harvesting, wells were trypsinized and counted in triplicate. Cell cycle analyses were performed using propidium iodide staining and FACS. For extracellular matrix invasion assays, Matrigel coated and noncoated cell inserts were used as specified by the manufacturer (Becton Dickinson, Bedford, MA).

To analyze the response of keratinocytes to growth factors, cells at 70%–80% confluence were incubated for 24 hr in serum/growth factor free media, and then stimulated by addition of insulin (10 μg/ml), IGF-1 (50 ng /ml), EGF (50 ng/ml), or fetal calf serum up to 15%. To inhibit the MAPK pathway, cells were grown in media containing 5 μg/ml PD98059 (Calbiochem) and the media was changed every 12 hr.

Ras Activity Measurements

Ras activity was measured by using a "pulldown assay" with a fusion protein of GST linked to the GTP-Ras binding domain of Raf1 (Herrmann et al., 1995). Briefly, epidermis was extracted with buffer [25 mM Hepes, pH 7.5, 150 mM NaCl, 1% NP40, 0.25% sodium deoxycholate, 10% glycerol, 25 mM NaF, 10 mM $MgCl_2$, 1 mM EDTA, 1 mM sodium orthovanadate] in the presence of a complete set of protease inhibitors (Roche, Indianapolis, IN). Total epidermal protein (500 μg) was combined with 10 μg of the GST-Raf1 fusion protein, and incubated for 2 hr at 4°C with rotation. A 50% slurry of glutathione-sepharose (50 μl) was added to each sample and incubated for an additional hour. After washing the beads four times with lysis buffer, bound GTP-Ras was released by boiling in 1 × SDS loading buffer, and after SDS-PAGE and immunoblotting, anti-panel-Ras antibodies were used to identify the protein.

MAPK (Erk1/2) Activity Measurements

SDS-PAGE and immunoblot analyses were used to identify the Erk1/2 proteins in epidermis or cultured keratinocytes. The active, i.e., phosphorylated, form of Erk1/2 was identified with anti-phospho-MAPK (Thr202/Tyr204) antibodies. A Molecular Dynamics Densitometer was used to quantitate the results.

Acknowledgments

We thank M. Yin for electron microscopy preparations, Dr. S. Tsukita for α-catenin cDNA, and Dr. J. L. Bos for the GST-RBD construct

for GTP-Ras pulldown assays. We thank G. Mundschau for ES cell injections and E. Hall for animal care. This work was supported by grants from the National Institutes of Health (R01-AR27883) and from the National Cancer Institute (5P50 DE11921). E. F. is an Investigator of the Howard Hughes Medical Institute.

Received July 17, 2000; revised January 29, 2001.

References

Adams, C.L., Chen, Y.T., Smith, S.J., and Nelson, W.J. (1998). Mechanisms of epithelial cell-cell adhesion and cell compaction revealed by high-resolution tracking of E-cadherin-green fluorescent protein. J. Cell Biol. *142*, 1105–1119.

Bagutti, C., Speight, P.M., and Watt, F.M. (1998). Comparison of integrin, cadherin, and catenin expression in squamous cell carcinomas of the oral cavity. J. Pathol. *186*, 8–16.

Balmain, A., and Harris, C.C. (2000). Carcinogenesis in mouse and human cells: parallels and paradoxes. Carcinogenesis *21*, 371–377.

Bullions, L.C., Notterman, D.A., Chung, L.S., and Levine, A.J. (1997). Expression of wild-type alpha-catenin protein in cells with a mutant alpha-catenin gene restores both growth regulation and tumor suppressor activities. Mol. Cell. Biol. *17*, 4501–4508.

Carmeliet, P., Lampugnani, M.G., Moons, L., Breviario, F., Compernolle, V., Bono, F., Balconi, G., Spagnuolo, R., Oostuyse, B., Dewerchin, M., et al. (1999). Targeted deficiency or cytosolic truncation of the VE-cadherin gene in mice impairs VEGF-mediated endothelial survival and angiogenesis. Cell *98*, 147–157.

Chan, T.O., Rittenhouse, S.E., and Tsichlis, P.N. (1999). AKT/PKB and other D3 phosphoinositide-regulated kinases: kinase activation by phosphoinositide-dependent phosphorylation. Annu. Rev. Biochem. *68*, 965–1014.

DasGupta, R., and Fuchs, E. (1999). Multiple roles for activated LEF/TCF transcription complexes during hair follicle development and differentiation. Development *126*, 4557–4568.

Drubin, D.G., and Nelson, W.J. (1996). Origins of cell polarity. Cell *84*, 335–344.

Espada, J., Perez-Moreno, M., Braga, V.M., Rodriguez-Viciana, P., and Cano, A. (1999). H-Ras activation promotes cytoplasmic accumulation and phosphoinositide 3-OH kinase association of beta-catenin in epidermal keratinocytes. J. Cell Biol. *146*, 967–980.

Freedberg, I.M., Eisen, A.Z., Wolff, K., Austen, K.F., Goldsmith, L.A., Katz, S.I., and Fitzpatrick, T.B. (1999). Dermatology in General Medicine, Fifth Edition, Volume I and II (New York: McGraw-Hill, Inc.).

Gallicano, G.I., Kouklis, P., Bauer, C., Yin, M., Vasioukhin, V., Degenstein, L., and Fuchs, E. (1998). Desmoplakin is required early in development for assembly of desmosomes and cytoskeletal linkage. J. Cell Biol. *143*, 2009–2022.

Guilford, P., Hopkins, J., Harraway, J., McLeod, M., McLeod, N., Harawira, P., Taite, H., Scoular, R., Miller, A., and Reeve, A.E. (1998). E-cadherin germline mutations in familial gastric cancer. Nature *392*, 402–405.

Gumbiner, B.M. (2000). Regulation of cadherin adhesive activity. J. Cell Biol. *148*, 399–404.

Hanahan, D., and Weinberg, R.A. (2000). The hallmarks of cancer. Cell *100*, 57–70.

Hardy, M.H. (1992). The secret life of the hair follicle. Trends Genet. *8*, 159–166.

Herrmann, C., Martin, G.A., and Wittinghofer, A. (1995). Quantitative analysis of the complex between p21ras and the Ras-binding domain of the human Raf-1 protein kinase. J. Biol. Chem. *270*, 2901–2905.

Higgins, J.M., Mandlebrot, D.A., Shaw, S.K., Russell, G.J., Murphy, E.A., Chen, Y.T., Nelson, W.J., Parker, C.M., and Brenner, M.B. (1998). Direct and regulated interaction of integrin alphaEbeta7 with E-cadherin. J. Cell Biol. *140*, 197–210.

Hirai, Y., Nose, A., Kobayashi, S., and Takeichi, M. (1989). Expression and role of E- and P-cadherin adhesion molecules in embryonic histogenesis. II. Skin morphogenesis. Development *105*, 271–277.

Hodivala, K.J., and Watt, F.M. (1994). Evidence that cadherins play a role in the downregulation of integrin expression that occurs during keratinocyte terminal differentiation. J. Cell Biol. *124*, 589–600.

Kinch, M.S., Clark, G.J., Der, C.J., and Burridge, K. (1995). Tyrosine phosphorylation regulates the adhesions of ras-transformed breast epithelia. J. Cell Biol. *130*, 461–471.

Kinzler, K.W., and Vogelstein, B. (1996). Lessons from hereditary colorectal cancer. Cell *87*, 159–170.

Kofron, M., Spagnuolo, A., Klymkowsky, M., Wylie, C., and Heasman, J. (1997). The roles of maternal alpha-catenin and plakoglobin in the early Xenopus embryo. Development *124*, 1553–1560.

Kowalczyk, A.P., Bornslaeger, E.A., Norvell, S.M., Palka, H.L., and Green, K.J. (1999). Desmosomes: intercellular adhesive junctions specialized for attachment of intermediate filaments. Int. Rev. Cytol. *185*, 237–302.

Larue, L., Ohsugi, M., Hirchenhain, J., and Kemler, R. (1994). E-cadherin null mutant embryos fail to form a trophectoderm epithelium. Proc. Natl. Acad. Sci. USA *91*, 8263–8267.

Macpherson, I. (1970). The characteristics of animal cells transformed in vitro. Adv. Cancer Res. *13*, 169–215.

Myers, M.G., Jr., Grammer, T.C., Wang, L.M., Sun, X.J., Pierce, J.H., Blenis, J., and White, M.F. (1994). Insulin receptor substrate-1 mediates phosphatidylinositol 3′-kinase and p70S6k signaling during insulin, insulin-like growth factor-1, and interleukin-4 stimulation. J. Biol. Chem. *269*, 28783–28789.

Nathke, I.S., Hinck, L., Swedlow, J.R., Papkoff, J., and Nelson, W.J. (1994). Defining interactions and distributions of cadherin and catenin complexes in polarized epithelial cells. J. Cell Biol. *125*, 1341–1352.

Nose, A., Nagafuchi, A., and Takeichi, M. (1988). Expressed recombinant cadherins mediate cell sorting in model systems. Cell *54*, 993–1001.

Ozawa, M., and Kemler, R. (1998). The membrane-proximal region of the E-cadherin cytoplasmic domain prevents dimerization and negatively regulates adhesion activity. J. Cell Biol. *21*, 1605–1613.

Perl, A.K., Wilgenbus, P., Dahl, U., Semb, H., and Christofori, G. (1998). A causal role for E-cadherin in the transition from adenoma to carcinoma. Nature *392*, 190–193.

Playford, M.P., Bicknell, D., Bodmer, W.F., and Macaulay, V.M. (2000). Insulin-like growth factor 1 regulates the location, stability, and transcriptional activity of beta-catenin. Proc. Natl. Acad. Sci. USA *97*, 12103–12108.

Rheinwald, J.G., and Green, H. (1975). Serial cultivation of strains of human epidermal keratinocytes: the formation of keratinizing colonies from single cells. Cell *6*, 331–343.

Shiozaki, H., Iihara, K., Oka, H., Kadowaki, T., Matsui, S., Gofuku, J., Inoue, M., Nagafuchi, A., Tsukita, S., and Mori, T. (1994). Immunohistochemical detection of alpha-catenin expression in human cancers. Am. J. Pathol. *144*, 667–674.

St. Croix, B., Sheehan, C., Rak, J.W., Florenes, V.A., Slingerland, J.M., and Kerbel, R.S. (1998). E-Cadherin-dependent growth suppression is mediated by the cyclin-dependent kinase inhibitor p27(KIP1). J. Cell Biol. *142*, 557–571.

Stoler, A., Kopan, R., Duvic, M., and Fuchs, E. (1988). The use of monospecific antibodies and cRNA probes reveals abnormal pathways of terminal differentiation in human epidermal diseases. J. Cell Biol. *107*, 427–446.

Sun, T.-T., Eichner, R., Schermer, A., Cooper, D., Nelson, W.G., and Weiss, R.A. (1984). The transformed phenotype. In The Cancer Cell, A. Levine, W. Topp, G.V.D. Woude, and A. J. D. Watson, eds. (Cold Spring Harbor, New York: Cold Spring Harbor Laboratory), pp. 169–176.

Torres, M., Stoykova, A., Huber, O., Chowdhury, K., Bonaldo, P., Mansouri, A., Butz, S., Kemler, R., and Gruss, P. (1997). An alpha-E-catenin gene trap mutation defines its function in preimplantation development. Proc. Natl. Acad. Sci. USA *94*, 901–906.

Uemura, T., Oda, H., Kraut, R., Hayashi, S., Kotaoka, Y., and Takeichi, M. (1996). Zygotic Drosophila E-cadherin expression is required for

processes of dynamic epithelial cell rearrangement in the Drosophila embryo. Genes Dev. *10*, 659–671.

Vasioukhin, V., Degenstein, L., Wise, B., and Fuchs, E. (1999). The magical touch: genome targeting in epidermal stem cells induced by tamoxifen application to mouse skin. Proc. Natl. Acad. Sci. USA *96*, 8551–8556.

Vasioukhin, V., Bauer, C., Yin, M., and Fuchs, E. (2000). Directed actin polymerization is the driving force for epithelial cell-cell adhesion. Cell *100*, 209–219.

von Schlippe, M., Marshall, J.F., Perry, P., Stone, M., Zhu, A.J., and Hart, I.R. (2000). Functional interaction between E-cadherin and alphav-containing integrins in carcinoma cells. J. Cell Sci. *113*, 425–437.

Wang, X., Zinkel, S., Polansky, K., and Fuchs, E. (1997). Marked growth enhancement in transgenic mice expressing keratin promoter-driven human growth hormone: implications for keratinocyte mediated gene therapy. Proc. Natl. Acad. Sci. USA *94*, 219–226.

Wang, X.J., Greenhalgh, D.A., and Roop, D.R. (2000). Transgenic coexpression of v-Ha-ras and transforming growth factor alpha increases epidermal hyperproliferation and tumorigenesis and predisposes to malignant conversion via endogenous c-Ha-ras activation. Mol. Carcinog. *27*, 200–209.

Watabe, M., Nagafuchi, A., Tsukita, S., and Takeichi, M. (1994). Induction of polarized cell-cell association and retardation of growth by activation of the E-cadherin-catenin adhesion system in a dispersed carcinoma line. J. Cell Biol. *127*, 247–256.

Yap, A.S. (1998). The morphogenetic role of cadherin cell adhesion molecules in human cancer: a thematic review. Cancer Invest. *16*, 252–261.

Yonemura, S., Itoh, M., Nagafuchi, A., and Tsukita, S. (1995). Cell-to-cell adherens junction formation and actin filament organization: similarities and differences between non-polarized fibroblasts and polarized epithelial cells. J. Cell Sci. *108*, 127–142.

Yuspa, S.H. (1998). The pathogenesis of squamous cell cancer: lessons learned from studies of skin carcinogenesis. J. Dermatol. Sci. *17*, 1–7.